Biophysical Chemistry, 35 (1990) 75–84
Elsevier

BIOCHE 01404

A fluorescence temperature-jump study on Ca^{2+}-induced conformational changes in calmodulin

Hirotsugu Tsuruta and Takayuki Sano

Department of Materials Science, Faculty of Science, Hiroshima University, Higashisenda-machi, Naka-ku, Hiroshima 730, Japan

Received 11 May 1989
Revised manuscript received 29 July 1989
Accepted 11 October 1989

Calmodulin; Temperature-jump; Chemical relaxation; Fluorescence; Conformational change; Kinetics

Calmodulin has been shown to alter its conformation so as to interact with a number of target proteins upon Ca^{2+} binding. A Ca^{2+}-binding study of calmodulin was performed by monitoring the fluorescence of intrinsic tyrosine residues and the probe 1-anilinonaphthalene-8-sulfonate (ANS). ANS fluorescence was shown to reflect Ca^{2+} binding to both high- and low-affinity sites. On the one hand, tyrosine fluorescence was sensitive only to the high-affinity Ca^{2+} binding. Temperature-jump investigation of the ternary complex of Ca^{2+}-calmodullin-ANS in combination with monitoring of ANS fluorescence demonstrated the kinetic characteristics of the conformational change. The relaxation process was attributed to Ca^{2+}-induced conformational change and the rate constants of this process were evaluated. On the basis of the rate constants of the conformational change, a rapid response of calmodulin in Ca^{2+} signaling is suggested.

1. Introduction

Calmodulin is a typical Ca^{2+}-binding protein possessing four Ca^{2+}-binding sites, of which two are of high affinity and two of low affinity. Each Ca^{2+}-binding site has the EF hand structure, i.e., a helix-loop-helix motif which is a common characteristic of the calmodulin superfamily of Ca^{2+}-binding proteins in eukaryotes [1] and which was found recently in a Ca^{2+}-binding protein of a prokaryote [2]. Ca^{2+}-binding proteins of the calmodulin superfamily have been considered as the most essential protein for living organisms. In particular, calmodulin has been extensively investigated, since the protein is quite ubiquitous and plays an important role in cellular Ca^{2+} signaling through interaction with a great many enzymes and cytoskeletal proteins in a Ca^{2+}-dependent manner [3,4]. Since the primary structure of calmodulin has remained conserved during evolution, an essential role is suggested for the protein in multifunctional regulation. The structure of calmodulin has been shown to be dumbbell-shaped in X-ray crystallographic studies [5,6]. The central, long α-helix connecting the two globular domains is considered to be an important factor in interactions with target proteins.

Although the mechanism of the multifunctional regulation remains obscure at the molecular level, the initial step during intracellular modulation by Ca^{2+}-calmodulin involves three molecular events in calmodulin: Ca^{2+} binding to each site, successive conformational change and interaction with target proteins. Equilibrium and flow dialysis

Correspondence address: T. Sano, Department of Materials Science, Faculty of Science, Hiroshima University, Higashisenda-machi, Naka-ku, Hiroshima 730, Japan.

0301-4622/90/$03.50 © 1990 Elsevier Science Publishers B.V. (Biomedical Division)

studies have been performed on the first, Ca^{2+}-binding, process and revealed two classes of Ca^{2+}-binding site: two high- and two low-affinity sites. Cooperative Ca^{2+} binding and the effect of metal ions such as Mg^{2+} on Ca^{2+} binding have also been reported [7–15]. Conformational changes in secondary and tertiary structure upon Ca^{2+} binding have been demonstrated in terms of circular dichroism [7,16,17], ^{1}H-NMR [18] and Raman spectroscopy [19]. A small-angle X-ray scattering study showed an increase in radius of gyration upon Ca^{2+} binding, presumably owing to the exposure of both ends of the central helix which were buried within the two globular lobes in the absence of Ca^{2+} [20].

Many target proteins and interactive polypeptides including peptide fragments of target proteins are known to form high-affinity complexes with calmodulin in a Ca^{2+}-dependent manner. Dissociation constants within the nanomolar range have been reported for the complexes [4,21–24]. A microcalorimetric study demonstrated entropy-driven complexation with the amphiphilic peptide melittin [25], suggesting that hydrophobic interaction is a dominant association factor. Conformational change accompanied by the exposure of hydrophobic regions in calmodulin has been shown to occur when Ca^{2+} binds to calmodulin, on the basis of ANS binding [26] and phenyl-Sepharose adsorption [27]. Thus, Ca^{2+}-induced exposure of the hydrophobic region, with which target proteins interact, may be important in the multifunctional regulation.

As for investigations on the kinetics of each molecular process for calmodulin, only those of the dissociation in the first Ca^{2+}-binding process have been studied extensively by means of a stopped-flow method. However, the association kinetics have not been observed due to the fast association rate [28–31]. It would be of great importance to establish the kinetic behavior of the conformational process in order to reveal the molecular mechanism of multifunctional regulation by calmodulin.

In this paper, we report a temperature-jump study of Ca^{2+}-induced conformational changes in calmodulin with the aid of ANS fluorescence detection, as well as Ca^{2+}- and ANS-binding studies.

2. Experimental

2.1. Materials

Bovine brain calmodullin was prepared through ion-exchange chromatography using DEAE-cellulofine (Seikagaku Kogyo, Tokyo), ammonium sulfate fractionation and isoelectric precipitation [32], followed by hydrophobic interaction chromatography employing phenyl-Sepharose CL-4B (Pharmacia, Upsala) [27]. Calmodulin was eluted from the phenyl-Sepharose column with buffer solution containing EGTA and then applied to a Sephadex G-25 column (Pharmacia) previously equilibrated with buffer solution (pH 7.4) containing 50 mM Hepes and 0.15 M NaCl in order to remove EGTA. Contaminating metal ions were further eliminated by passage through a Unicellex chelating resin column (Dojin, Kumamoto) equilibrated with the Hepes buffer solution.

The calmodulin thus obtained migrated as a single band on SDS-polyacrylamide gel electrophoresis [33]. No impurity containing tryptophan residues was detectable in terms of the fluorescence spectrum. The calmodulin concentration was determined spectrophotometrically using an extinction coefficient of $E^{1\%}_{280\ nm} = 2.0$ for Ca^{2+}-free calmodulin and a molecular weight of 16680 [34]. All reagents were of guaranteed grade or better.

2.2. Steady-state fluorescence

Fluorescence measurements at equilibrium were performed on a Shimadzu RF-540 spectrofluorometer. Excitation wavelengths were 285 and 360 nm for tyrosine and ANS, respectively. In titration experiments, the intensities of the emitted fluorescence were measured at 310 and 480 nm for tyrosine and ANS, respectively. All fluorescence data were subjected to dilution correction and backgrond subtraction. In the case of ANS titration of calmodulin, attenuation of ANS fluorescence due to inner filter effects was corrected according to the procedure reported by Holland et al. [35].

Fluorescence titration curves were analyzed on the basis of the following equation, deduced for fluorescence change assuming equivalent binding

sites and constant fluorescence change by each ligand binding [36]:

$$\frac{1}{(1-\theta)K_A} = \frac{[X]_T}{\theta} - p[A]_T \quad (1)$$

with $\theta = \Delta F/\Delta F_{max}$

where $[X]_T$ designates the total concentration of ligand X, $[A]_T$ total concentration of acceptor A, p number of binding sites per acceptor, K_A binding constant, ΔF change in fluorescence intensity and ΔF_{max} maximum fluorescence change, i.e., the fluorescence intensity of the ligand-saturated acceptor.

Titration data were also analyzed by curve fitting to the following binding scheme with an iterative nonlinear least-squares method employing the Marquardt algorithm [37]. For the stepwise binding scheme with respective binding constants K_i:

$$A \underset{K_1}{\overset{X}{\rightleftharpoons}} AX \underset{K_2}{\overset{X}{\rightleftharpoons}} AX_2 \ldots AX_{n-1} \underset{K_n}{\overset{X}{\rightleftharpoons}} AX_n,$$

the Klotz binding function, i.e. the fractional saturation was defined as

$$\frac{K_1[X] + 2K_1K_2[X]^2 + \ldots + nK_1K_2 \ldots K_n[X]^n}{1 + K_1[X] + K_1K_2[X]^2 + \ldots + K_1K_2 \ldots K_n[X]^n} \quad (2)$$

where the concentration [X] was calculated from the total concentrations of ligand and acceptor. In this analysis, fractional saturation was assumed to be proportional to the fluorescence change $\Delta F/\Delta F_{max}$. Association constants K_i were evaluated by the nonlinear least-squares method.

2.3. Fluorescence temperature jump

Kinetic measurements were performed by means of a laboratory-made temperature-jump apparatus [38] improved for fluorescence detection. This apparatus provides a temperature jump of 9 K within 5 μs by joule heating under the present experimental conditions. A sample solution containing ANS was irradiated with monochromatized ultraviolet light (365 nm) from a high-pressure mercury lamp and changes in ANS fluorescence intensity were measured at right angles. Scattered incident light was eliminated with low-cut filter (Toshiba L-39). The time constant of the detection circuit was 3.3 μs. Kinetic data were digitized and analyzed on a microcomputer.

All measurements were performed at 20 °C and buffer solution 50 mM Hepes (pH 7.4) containing 0.15 M NaCl was used throughout.

3. Results

3.1. Fluorescence titration study of Ca^{2+} binding

Ca^{2+} binding increased the fluorescence intensity of tyrosine (fig. 1). The association constant, $(3.40 \pm 0.06) \times 10^5$ M^{-1}, and number of binding sites, 2.05 ± 0.01, were evaluated from a plot based on eq. 1. This result suggests the existence of two Ca^{2+}-binding sites corresponding to the high-affinity sites as determined in direct Ca^{2+}-binding studies [7–13]. Thus, tyrosine fluorescence was shown to be a probe for high-affinity Ca^{2+} binding to calmodulin, while four Ca^{2+}-binding sites are widely accepted as for calmodulin. Accordingly, in order to estimate more reliable associa-

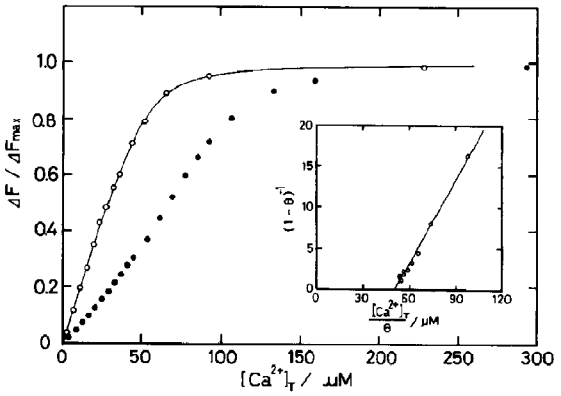

Fig. 1. Ca^{2+} titration curves as monitored by tyrosine (○) and ANS (●) fluorescence at concentrations of 25 μM calmodulin and 200 μM ANS. (Inset) Plot based on eq. 1 of the former titration data. (———) Fitting curve based on the stepwise Ca^{2+}-binding scheme with use of the four binding constants in the text.

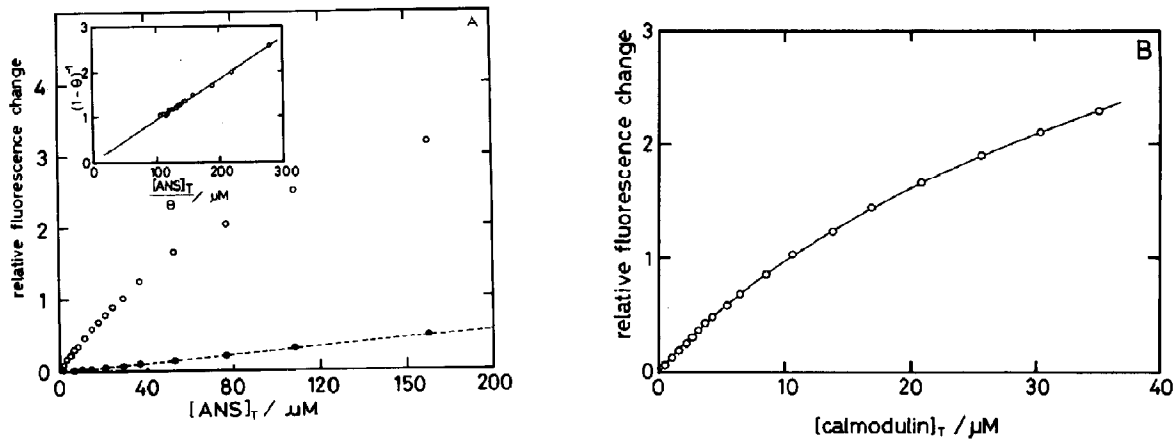

Fig. 2. (A) ANS titration curve in the presence of 0.5 mM Ca^{2+} (○) and absence of Ca^{2+} (●). Calmodulin concentration, 2.02 μM. (------) Basal level of non-Ca^{2+}-specific fluorescence change. (Inset) Plot based on eq. 1 of the difference titration data. Fluorescence intensities were corrected for inner filter effects. (B) Calmodulin titration curve. Ca^{2+} and ANS concentrations: 1 mM and 10 μM, respectively. (———) Fitting curve with $K_{ANS} = 3.86 \times 10^4$ M^{-1} and $p = 4$.

tion constants, the iterative curve fitting analysis was carried out by considering the contribution from two additional low-affinity Ca^{2+}-binding sites, which do not affect tyrosine fluorescence because of their location at a distance from the two tyrosine residues in the C-terminal half. Starting with the binding constant cited above as an initial value for the two high-affinity binding constants, and with a value one order smaller than the initial value for the two low-affinity binding constants, four Ca^{2+}-binding constants were obtained via the curve fitting analysis: $K_1 = (4.35 \pm 1.21) \times 10^5$ M^{-1}, $K_2 = (3.72 \pm 0.68) \times 10^5$ M^{-1}, $K_3 = (2.76 \pm 0.95) \times 10^4$ M^{-1} and $K_4 = (1.81 \pm 1.28) \times 10^4$ M^{-1}. K_3 and K_4 were not determined unambiguously because the lower the affinity, the lesser was the effect on the fluorescence Ca^{2+}-binding curve. The present result is consistent with those determined through different methods [7,8,14,39].

In addition, Ca^{2+} binding was monitored by ANS fluorescence. Ca^{2+} binding enhanced ANS fluorescence as shown in fig. 1, suggesting the Ca^{2+}-induced exposure of ANS-binding sites on the protein. In a parallel experiment, tyrosine fluorescence was monitored with addition of Ca^{2+} in the presence of ANS (data not shown). Although the fluorescence intensity of tyrosine was very low due to absorption of excitation and emission light by ANS, a Ca^{2+}-binding curve rather similar to that in the absence of ANS was obtained. This fact demonstrates that the Ca^{2+}-binding affinity is unaltered on ANS binding to calmodulin. An approx. 2-fold greater total concentration of Ca^{2+} was required to saturate ANS fluorescence as compared with tyrosine fluorescence.

We tried to simulate the ANS-detectable Ca^{2+}-binding curve in order to estimate the low-affinity Ca^{2+}-binding constants, but perfect simulation of the binding curve was impossible due to the lack of data on the respective ANS-binding constants for the calmodulin species: CaM, $CaMCa_1$, $CaMCa_2$, $CaMCa_3$ and $CaMCa_4$. The simulation curve with respect to only the two high-affinity sites was inconsistent with the ANS-detectable Ca^{2+}-binding curve regardless of the value assumed for the homogeneous ANS-binding constant and was rather similar to the high-affinity binding curve as measured by tyrosine fluorescence. Thus, the low-affinity Ca^{2+}-binding sites might contribute to the ANS-detectable Ca^{2+}-binding curve. A stopped-flow study, in which the kinetics of dissociation of Ca^{2+} from the high- and low-affinity sites was observed in biphasic ANS fluorescence decay, also provides evidence in support of a contribution arising from the low-affinity sites to ANS fluorescence [29]. Conse-

quently, in the following kinetic analysis we consider ANS fluorescence to be a reliable means of detecting Ca^{2+}-induced conformational changes in the proximity of both high- and low-affinity Ca^{2+}-binding sites.

3.2. Fluorescence titration study of ANS binding

Fig. 2A shows a plot of ANS binding as monitored by the enhancement of ANS fluorescence. The fluorescence intensity was significantly enhanced with increasing ANS concentration in the presence of excess Ca^{2+}, whereas the increase, although still linear, was only to a very small extent, in the absence of Ca^{2+}. This is indicative of the interaction between ANS and calmodulin in the absence of Ca^{2+} being very weak. This non-Ca^{2+}-specific fluorescence change of ANS was subtracted from each data point prior to further analysis. Although the maximum change in fluorescence intensity ΔF_{max} was not directly observable in this titration experiment, the association constant for ANS binding to Ca^{2+}-saturated calmodulin was estimated to be $K_{ANS} = (9.0 \pm 0.8) \times 10^3\ M^{-1}$ from a plot based on eq. 1 with ΔF_{max} as adjustable parameter. The number of ANS-binding sites could not be unambiguously determined in this analysis due to uncertainty in the maximum level. The fluorescence data were corrected for inner filter effects, however, non-Ca^{2+}-specific interaction of ANS with calmodulin might be crucial at high concentrations of ANS.

Reverse calmodulin titration was carried out at lower ANS concentrations in order to obtain a more reliable value for the ANS-binding constant, since it is free from inner filter effects and the influence of nonspecific ANS- binding (fig. 2B). A plot based on eq. 1 provided a value for the association constant similar to that cited above, while the number of binding sites, p, was not unequivocally determined, since the saturation level of ANS fluorescence was not measured. Curve-fitting analyses were carried out. Unfortunately, fittings for $p = 2$–4 were very similar within the accessible region of the binding curve, however, more reliable binding constants, K_{ANS} values, within the range 2.91–$3.86 \times 10^4\ M^{-1}$ were obtained, which were free from nonspecific ANS-binding effects and thus were used in further analysis.

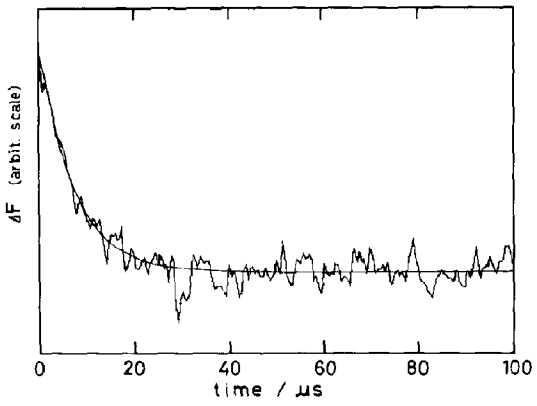

Fig. 3. Typical temperature-jump relaxation kinetics monitored by ANS fluorescence under condition of 20.2 μM calmodulin, 2 mM Ca^{2+} and 50 μM ANS ($T = 9$ K). 23 kinetic traces were averaged. Smooth trace: fitting curve based on a single-exponential decay, yielding a time constant of (29.6 ± 1.3) μs.

3.3. Fluorescence temperature-jump

The relaxation curve for the ternary complex, Ca^{2+}-calmodulin-ANS, indicated apparently single-exponential behavior of the fluorescence decay (fig. 3). The time courses had a low signal-to-noise ratio such that resolution into multiple exponential components was not possible. No relaxation was detected in the absence of Ca^{2+}, suggesting that Ca^{2+} binding is essential for this relaxation process. The transient decrease in ANS fluorescence intensity caused by a temperature-jump was consistent with the temperature dependence of the fluorescence spectrum of the ternary complex (data not shown), showing that ANS-binding and/or Ca^{2+}-binding equilibrium is/are shifted toward ANS dissociation from Ca^{2+}-ligated calmodulin by a temperature-jump.

The concentration dependence of the relaxation time (fig. 4) could be accounted for by a model scheme considering the three probable molecular events in Ca^{2+}-binding domains: Ca^{2+} binding, conformational change accompanied by exposure of ANS-binding sites and ANS binding to the sites with increasing fluorescence quantum yield.

Cooperative Ca^{2+} binding of calmodulin has been reported by many investigators, however, a consensus regarding the properties has not been reached [11]. Thus, for simplicity, four Ca^{2+}-binding sites were considered to be independent and to be of equal affinity. One ANS-binding site of a hydrophobic nature was assumed to be present in each Ca^{2+}-binding domain. We then consider the following scheme for all four Ca^{2+}-binding domains:

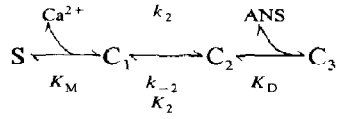

Scheme 1.

where S represents a Ca^{2+}-binding domain, C_1 a Ca^{2+}-ligated domain, C_2 a Ca^{2+}-ligated domain with an exposed ANS-binding site, C_3 a domain with a bound ANS, K_M the binding constant of the metal ion, K_2 the equilibrium constant for the intramolecular conformational change which could not be evaluated experimentally and was the only adjustable parameter in the following analysis, K_D the binding constant of the fluorescent probe, and k_2 and k_{-2} the rate constants of the conformational change with the relationship $K_2 = k_2/k_{-2}$. The binding constants K_M and K_D can be obtained from the apparent binding constants determined in the fluorescence titration studies:

$$K_M = \frac{K_{Ca}}{1 + K_2} \tag{3}$$

$$K_D = K_{ANS}\frac{K_2 + 1}{K_2}\frac{K_{Ca}[Ca]_0 + 1}{K_{Ca}[Ca]_0} \tag{4}$$

where K_{Ca} designates the apparent Ca^{2+}-binding constant, and K_{ANS} the apparent ANS-binding constant determined at a Ca^{2+} concentration, $[Ca]_0$, which is approximately equal to the total Ca^{2+} concentration under the present conditions. K_{Ca} was assumed to have the value 9.48×10^4 M^{-1}, which is the geometric mean of the association constants of the two high-affinity (4.35×10^5 and 3.72×10^5 M^{-1}) and two low-affinity (2.76×10^4 and 1.81×10^4 M^{-1}) sites. The K_{ANS} value employed was 3.86×10^4 M^{-1}, which was determined via curve fitting analysis with the assumption of $p = 4$.

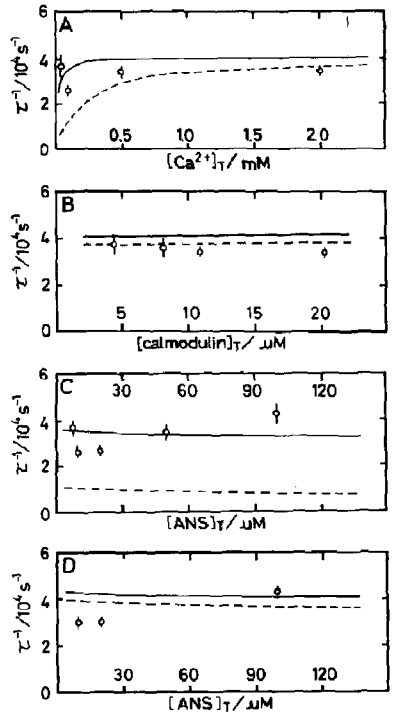

Fig. 4. Concentration dependence of the relaxation time. (A) Ca^{2+} dependence at 10.85 μM calmodulin and 50 μM ANS. (B) calmodulin dependence at 2 mM Ca^{2+} and 50 μM ANS. (C) ANS dependence at 9.88 μM calmodulin and 80 μM Ca^{2+}. (D) ANS dependence at 10.85 μM calmodulin and 2 mM Ca^{2+}. Solid and broken curves represent the calculated concentration dependence of relaxation time for (———) high-affinity and (— — —) low-affinity Ca^{2+}-binding domain, according to eq. 6 using the equilibrium and rate constants evaluated.

We examined the Ca^{2+}-binding and/or ANS-binding process in scheme 1 as a possible explanation for the observed relaxation process. However, neither binding process satisfied the experimentally observed dependence on concentration of the relaxation time. Among a wide variety of reaction schemes examined, the observed relaxation process could be attributed to the intramolecular conversion in scheme 1, i.e., the conformational change in the Ca^{2+}-binding domain accompanied by the exposure of hydrophobic ANS-binding sites. The relaxation time for the intramolecular conversion

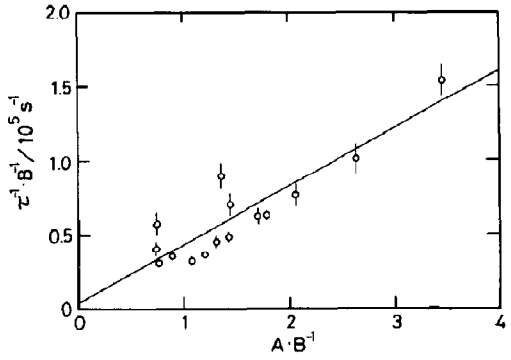

Fig. 5. Analysis of relaxation data based on eq. 5. Rate constants $k_2 = (3.9 \pm 0.4) \times 10^4\ s^{-1}$ and $k_{-2} = (3.8 \pm 5.9) \times 10^3\ s^{-1}$ were determined from the slope and the intercept, respectively, with the parameter $K_2 = 2.63$.

process is expressed as follows, provided that both the Ca^{2+}- and ANS-binding processes attain equilibrium rapidly relative to the intramolecular process [40]:

$$\tau^{-1} = k_2 \frac{[S] + [Ca^{2+}]}{K_M + [S] + [Ca^{2+}]} + k_{-2} \frac{K_D + [C_2]}{K_D + [C_2] + [ANS]} = k_2 A + k_{-2} B \quad (5)$$

In eq. 5, each of the concentrations could be evaluated from the total concentrations of calmodulin, Ca^{2+} and ANS with the constants K_M, K_D and K_2. A plot of τ^{-1}/B vs. A/B should give a straight line yielding the rate constants k_2 and k_{-2} from the slope and intercept, respectively. With the aid of the linearity of the plot and self-consistency in the parameter K_2, the reaction scheme was examined for many different values of K_2. Fig. 5 shows the plot for $K_2 = 2.63$. The rate constants were determined as $k_2 = (3.9 \pm 0.4) \times 10^4\ s^{-1}$ and $k_{-2} = (3.8 \pm 5.9) \times 10^3\ s^{-1}$. Good linearity in this plot suggests the validity of intramolecular conformational change as being the relaxation process.

4. Discussion

Calmodulin modulates many cellular functions in a Ca^{2+}-dependent manner through the three essential molecular events: Ca^{2+} binding, successive conformational change and interaction with target proteins. The temperature-jump relaxation process is attributed to a conformational change in calmodulin followed by exposure of the ANS-binding sites. It has been shown that the Ca^{2+}-induced conformational change in calmodulin is accompanied by hydrophobic amino acid residues becoming exposed at the protein's surface [26,27]. It is likely that hydrophobic interactions play an important role in the interaction with target proteins [25].

LaPorte et al. [26] showed in an equilibrium dialysis study that ANS binding to the exposed hydrophobic region of calmodulin induced a significant increase in ANS fluorescence, estimating the binding stoichiometry to be 2.1 ANS-binding sites per calmodulin molecule, with a dissociation constant of 490 μM.

We employed a fluorescent probe, ANS, to probe conformational changes in calmodulin and characterized a larger number of ANS-binding sites of higher affinity. This discrepancy may arise from differences in the Ca^{2+} concentration employed as well as in the methods followed. Under their experimental conditions, calmodulin cannot be saturated with Ca^{2+}; calmodulin species without Ca^{2+}, and ligated to one, two, three and four Ca^{2+} are calculated to be present in the respective proportions of 40.5, 27.4, 27.4, 4.5 and 0.2% at total concentrations of 0.1 mM calmodulin and 0.1 mM Ca^{2+}, with the use of values for the binding constants of $K_1 = 1.9 \times 10^5\ M^{-1}$, $K_2 = 2.8 \times 10^5\ M^{-1}$, $K_3 = 4.5 \times 10^4\ M^{-1}$ and $K_4 = 1.2 \times 10^4\ M^{-1}$ [14]. Thus, they might have measured the averaged affinity of Ca^{2+}-specific and non-Ca^{2+}-specific ANS-binding sites, since the hydrophobic ANS-binding sites could not be exposed entirely in terms of occupancy of Ca^{2+}-binding sites. This is supported by the present result of an ANS-binding constant greater by a factor of 2.6 being estimated in the calmodulin titration study at low ANS concentrations, as compared to the ANS titration study employing

high ANS concentrations. Recently, association constants of 2.8×10^5–9.1×10^6 M^{-1} were reported for ANS binding to bovine serum albumin [41]. ANS-binding affinity is probably strongly dependent on the properties of the binding sites, such as the hydrophobicity and electrostatic nature of the amino acid residues incorporated into the ANS-binding sites as well as the hydration with them.

We have considered the ANS-binding sites to possess a hydrophobic nature according to previous studies by various authors, however, we do not have sufficient knowledge to be able to conclude unambiguously that the exposed ANS-binding sites are hydrophobic. It was previously shown that the fluorescence enhancement induced by ANS binding to protein could be due to binding either to hydrophobic sites or to sites where local dipoles do not undergo relaxation during the excited-state lifetime of ANS [42].

A stopped-flow study with monitoring of ANS fluorescence demonstrated Ca^{2+} dissociation accompanying the biphasic decay of ANS fluorescence when ligated Ca^{2+} was chelated by EDTA [29]. Quite similar biphasic Ca^{2+} dissociation kinetics were also observed in stopped-flow studies in which changes in Ca^{2+} concentration were monitored directly through the change in fluorescence of the Ca^{2+} chelator quin-2 [30,31]. The authors attributed this kinetic behavior to Ca^{2+} dissociation from the two types of Ca^{2+}-binding site. These data suggest that ANS molecules bind to the two high- and two low-affinity Ca^{2+}-binding domains. In the present experiments, ANS fluorescence was shown to be sensitive to both low-affinity and high-affinity sites (fig. 1). The behavior of the temperature-jump kinetics of the ternary complex, Ca^{2+}-calmodulin-ANS, could be attributed to intramolecular conformational changes in calmodulin accompanied by the exposure of the hydrophobic region. The rate constants for this process, k_2 and k_{-2}, were determined based on the assumption of four homogeneous Ca^{2+}-binding sites. Positive cooperativity was reported to occur for Ca^{2+} binding by several researchers [7,11,14,15], however, we treat the four Ca^{2+}-binding sites as being independent in the kinetic analysis, since: (1) No such Ca^{2+}-binding feature was apparent in the present fluorescence titration; (2) the Ca^{2+}-binding property must be strongly dependent on the solution conditions. All previous studies postulating cooperativity were not carried out under conditions identical to those in the present work; (3) Ca^{2+} binding to the high-affinity sites might show positive cooperativity however, these sites were considered to be fully occupied at the lowest Ca^{2+} concentration employed in the present temperature-jump study.

The consensus of knowledge on Ca^{2+}-binding properties is considered to rest on the existence of the two high- and two low-affinity Ca^{2+}-binding sites. Hence, the entire reaction may be expressed more realistically as follows:

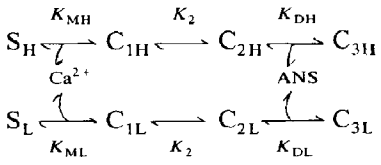

Scheme 2.

where subscripts H and L designate high- and low-affinity Ca^{2+}-binding domains, respectively.

The association/dissociation processes of Ca^{2+} and ANS were assumed to reach equilibrium very rapidly as depicted in scheme 1, in accordance with the facts that the Ca^{2+}-binding kinetics were too fast to be followed by stopped-flow methods [28–31], and that the diffusion-controlled rate constants for ANS binding to bovine serum albumin were reported [41]. K_{MH} and K_{ML} were calculated using the high- and low-affinity Ca^{2+}-binding constants as determined in the titration studies. The relaxation times for the two conformational changes in the high- and low-affinity Ca^{2+}-binding domains were derived as functions of the equilibrium constants and equilibrium concentrations in the same way as described above:

$$\tau_i^{-1} = k_2 \frac{[S_i] + [Ca^{2+}]}{K_{Mi} + [S_i] + [Ca^{2+}]} + k_{-2} \frac{K_D + [C_{2i}]}{K_D + [C_{2i}] + [ANS]} \quad (6)$$

where subscript i denotes high-affinity (H) or

low-affinity (L) Ca^{2+}-binding domains. The rate constants, k_2 and k_{-2} are assumed to be identical for both types of binding domain, owing to the rather high degree of homology in primary structures among the four Ca^{2+}-binding domains. The two relaxation times for both types of domain were evaluated on the basis of the rate constants obtained and plotted vs. total concentrations (fig. 4). At high Ca^{2+} concentrations, the relaxation times for the conformational changes in the high-affinity and low-affinity domains are very similar, and are consistent with the experimental findings. In contrast, at low Ca^{2+} concentrations, only the relaxation times calculated for the high-affinity domains coincide with the results (fig. 4A and C). This suggests that the intramolecular conformational change in the high-affinity Ca^{2+}-binding domains is the dominant relaxation component in the present temperature-jump study. ^{1}H-NMR and stopped-flow studies on calmodulin and its tryptic fragments provided thermodynamic parameters on the conformational changes and the dissociation of Ca^{2+}, showing that the activation parameter $\Delta H^{\ddagger}$ for the high-affinity domain was greater than that of the low-affinity domain by a factor of 1.5–2.2 irrespective of whether intact calmodulin or tryptic fragments were used [18,30]. This fact supports the present conclusion that the conformational change in the high-affinity domains is a major relaxation process. Thus, our simple approach has revealed the essential kinetic characteristics of the conformational change. A stricter analysis considering cooperativity and heterogeneity in Ca^{2+} binding seems difficult, since the concentration dependence of the relaxation time is not clearly evident.

Calmodulin must respond to transient Ca^{2+} signaling in vivo. The elucidation of its response is a matter of great importance and several studies have been performed in order to measure the Ca^{2+}-binding rate. A stopped-flow study monitoring tyrosine fluorescence was performed in an attempt to observe the kinetics of Ca^{2+} binding, however, the rate was too rapid to be followed [28]. To date, only the kinetics of dissociation have been studied [28–31]. We performed a temperature-jump investigation in order to ascertain the kinetic behavior of the conformational changes in calmodulin. The rate constants of $k_2 = (3.9 \pm 0.4) \times 10^4$ s^{-1} and $k_{-2} = (3.8 \pm 5.9) \times 10^3$ s^{-1} evaluated for the rate-determining conformational change suggest that the overall association rate of Ca^{2+} is beyond the ability of the stopped-flow method and that calmodulin is capable of responding within 1 ms to changes in the cytosolic Ca^{2+} concentration.

References

1 R.H. Kretsinger and C.E. Nockolds, J. Biol. Chem. 248 (1973) 3311.
2 D.G. Swan, R.S. Hale, N. Dhillon and P.F. Leadlay, Nature 329 (1987) 84.
3 C.B. Klee, T.H. Crouch and P.G. Richman, Ann. Rev. Biochem. 49 (1980) 489.
4 A.S. Manalan and C.B. Klee, Adv. Cyclic Nucleotides Protein Phosphorylation Res. 18 (1984) 227.
5 Y.S. Babu, J.S. Sack, T.J. Greenhough, C.E. Bugg, A.R. Means and W.J. Cook, Nature 315 (1985) 37.
6 R.H. Kretsinger, S.E. Rudnick and L.J. Weismann, J. Inorg. Biochem. 28 (1986) 289.
7 T.M. Crouch and C.B. Klee, Biochemistry 19 (1980) 3692.
8 J. Haiech, C.B. Klee and J.G. Demaille, Biochemistry 20 (1981) 3890.
9 M. Milos, J.J. Schaer, M. Comte and J.A. Cox, Biochemistry 25 (1986) 6279.
10 J.S. Mills and J.D. Johnson, J. Biol. Chem. 260 (1985) 15100.
11 J.A. Cox, Biochem. J. 249 (1988) 621.
12 B.B. Olwin, A.E. Edelman, E.G. Krebs and D.R. Strom, J. Biol. Chem. 259 (1984) 10949.
13 B.B. Olwin and D.R. Strom, Biochemistry 24 (1985) 8081.
14 C.H. Keller, B.B. Olwin, D.C. Laporte and D.R. Storm, Biochemistry 21 (1982) 156.
15 S. Iida and D. Potter, J. Biochem. (Tokyo) 99 (1986) 1765–1772.
16 W. Drabikowski, H. Brzeska and S.Y. Vernyamikov, J. Biol. Chem. 257 (1982) 11584.
17 R.E. Reid, Biochemistry 26 (1987) 6070.
18 M. Ikura, Biochim. Biophys. Acta 872 (1986) 195.
19 B.A. Seaton, J.E. Head, R.C. Lord and G.A. Petsko, Biochemistry 22 (1983) 973.
20 B.A. Seaton, J.F. Head, D.M. Engelman and F.M. Richards, Biochemistry 24 (1985) 6740.
21 J.A. Cox, M. Comte, J.E. Fitton and W.E. DeGrado, J. Biol. Chem. 260 (1985) 2527.
22 B. Buschmeier, H.E. Meyer and G.W. Mayr, J. Biol. Chem. 262 (1987) 9454.
23 C.Y. Huang, V. Chau, P.B. Chock, J.H. Wang and R.K. Sharma, Proc. Natl. Acad. Sci. U.S.A. 78 (1981) 871.
24 C.Y. Huang and M.M. King, Curr. Top. Cell. Regul. 27 (1985) 437.

25 M. Milos, J.J. Schaer, M. Comte and J.A. Cox, J. Biol. Chem. 262 (1987) 2746.
26 D.C. LaPorte, B.M. Wieman and D. Strom, Biochemistry 19 (1980) 3814.
27 R. Gopalakrishna and W.B. Anderson, Biochem. Biophys. Res. Commun. 104 (1982) 830.
28 D.A. Malencik, S.R. Anderson, Y. Shalitin and M.I. Schimerlik, Biochem. Biophys. Res. Commun. 101 (1981) 390.
29 P. Bayley, P. Ahlstrom, S.R. Martin and S. Forsen, Biochem. Biophys. Res. Commun. 120 (1984) 185.
30 S.R. Martin; A. Andersson Teleman, P.M. Bayley, M.T. Drakenberg and S. Forsen, Eur. J. Biochem. 151 (1985) 543.
31 J. Suko, W. Wyskovsky, J. Pidlich, R. Hauptner, B. Plank and G. Hellman, Eur. J. Biochem. 159 (1986) 425.
32 D. Guerini, J. Krebs and E. Carafoli, J. Biol. Chem. 259 (1984) 15172.
33 U.K. Laemmli, Nature 227 (1970) 680.
34 D.M. Watterson, W.G. Harrelson, Jr., P.M. Keller, F. Sharief and T.C. Vanaman, J. Biol. Chem. 251 (1976) 4501.
35 J.F. Holland, R.E. Teets, P.M. Kelly and A. Timnick, Anal. Chem. 49 (1977) 706.
36 R.A. Stinson and J.J. Holbrook, Biochem. J. 131 (1973) 719.
37 K. Yamaoka and K. Suzuki, Information 7 (1986) 36 (in Japanese).
38 S. Inoue, M. Nishimura, T. Yasunaga, H. Takemoto, and Y. Toyoshima, J. Phys. Chem. 85 (1981) 1401.
39 Y. Maulet and J.A. Cox, Biochemistry 22 (1983) 5680.
40 H. Strehlow and W. Knoche, Fundamentals of chemical relaxation. Monographs in modern chemistry, vol. 10 (Verlag Chemie, Weinheim, 1977).
41 P. Regenfuss and R.M. Clegg, Biophys. Chem. 26 (1987) 83.
42 J.D. Johnson, M.A. El-Bayoumi, L.D. Weber and A. Tulinsky, Biochemistry 18 (1979) 1292.